




Differential densimetry: A method for determining ultra-low fluid flux and tissue permeability

Cite as: AIP Advances 9, 095063 (2019); <https://doi.org/10.1063/1.5122953>

Submitted: 01 August 2019 . Accepted: 19 September 2019 . Published Online: 27 September 2019

Christopher S. Hale , Heran C. Bhakta, Carrie R. Jonak, Jennifer M. Yonan, Devin K. Binder, William H. Grover , and V. G. J. Rodgers 



View Online



Export Citation



CrossMark



NEW

AVS Quantum Science

A high impact interdisciplinary journal for **ALL** quantum science

ACCEPTING SUBMISSIONS

Differential densimetry: A method for determining ultra-low fluid flux and tissue permeability

Cite as: AIP Advances 9, 095063 (2019); doi: 10.1063/1.5122953

Submitted: 1 August 2019 • Accepted: 19 September 2019 •

Published Online: 27 September 2019



Christopher S. Hale,¹ Heran C. Bhakta,¹ Carrie R. Jonak,² Jennifer M. Yonan,² Devin K. Binder,² William H. Grover,¹ and V. G. J. Rodgers^{1,a)}

AFFILIATIONS

¹Department of Bioengineering, University of California, Riverside, Riverside, California 92521, USA

²Division of Biomedical Sciences, School of Medicine, University of California, Riverside, Riverside, California 92521, USA

^{a)}To whom correspondence should be addressed: Telephone: 951-827-4311, Facsimile: 951-827-6416, E-mail: victor.rodgers@ucr.edu

ABSTRACT

Osmotic transport devices (OTDs) are forward osmosis membrane devices that we recently developed to remove accumulated fluid from swollen tissue, *in-vivo*, under severe conditions. As such, the relative volume of the fluid required to be removed and the volumetric flowrate may be two orders of magnitude less than the operating volume and tangential flowrate of the device. This makes it challenging to measure the rate of fluid flow from the swollen tissue. Here, we introduce a differential densimetry method for determining ultra-low volumetric flux through tissue samples. This technique uses two vibrating tube density sensors, one placed upstream of the membrane in contact with the tissue sample, and one placed downstream. Any flow of biological fluid withdrawn through the tissue will combine with the OTD operating fluid resulting in an observed density shift in the second density sensor. By measuring the difference in density between the upstream and downstream fluids, one can calculate the amount of fluid flowing across the tissue with a relatively high level of sensitivity. This method is also relatively insensitive to drift from temperature fluctuations and capable of continuously monitoring tissue permeability in real time. As a proof of concept, we used this technique to measure fluid flow across *ex-vivo* rat spinal tissue for an appropriately scaled OTD. The repeatability error had a maximum of only 12%. This implies that this method can provide highly acceptable flux measurements with reasonable reproducibility in real-time applications of fluid removal *in-vivo*.

© 2019 Author(s). All article content, except where otherwise noted, is licensed under a Creative Commons Attribution (CC BY) license (<http://creativecommons.org/licenses/by/4.0/>). <https://doi.org/10.1063/1.5122953>

INTRODUCTION

Recently, forward osmosis membrane processes termed osmotic transport devices (OTD) have been shown to have tremendous success in removing fluid from biological tissue with edema associated with traumatic brain injury (TBI) and spinal cord injury (SCI).^{1,2} The general operation of the device consists of placing a semipermeable membrane process across a hydrogel that is applied directly on the swollen tissue (Figure 1). The hydrogel acts as a medium for continuous fluid contact between the device and the tissue. The process contains an impermeable osmolyte such as a protein that passes tangentially across the membrane. The resulting osmotic pressure provides a driving

force to expel permeable fluid in the tissue from the body into the OTD.

The OTD is based on standard tangential ultrafiltration technology where the flux, J_v , normal through the membrane is given by the Kedem-Katchalsky model:³

$$J_v = \frac{1}{\mu} \frac{\Delta P - \sigma_{osmolyte} \Delta \pi_{osmolyte}}{R_m + R_{membrane\ support} + R_{hydrogel} + R_{tissue}} \quad (1)$$

where ΔP is the transmembrane pressure, $\Delta \pi_{osmolyte}$ is the osmotic pressure due to the osmolyte, $\sigma_{osmolyte}$ is the osmotic reflection coefficient, R_m is the OTD membrane resistance, $R_{membrane\ support}$ is the flux resistance due to the OTD membrane support, $R_{hydrogel}$ is the

Osmotic Transport Device (OTD)

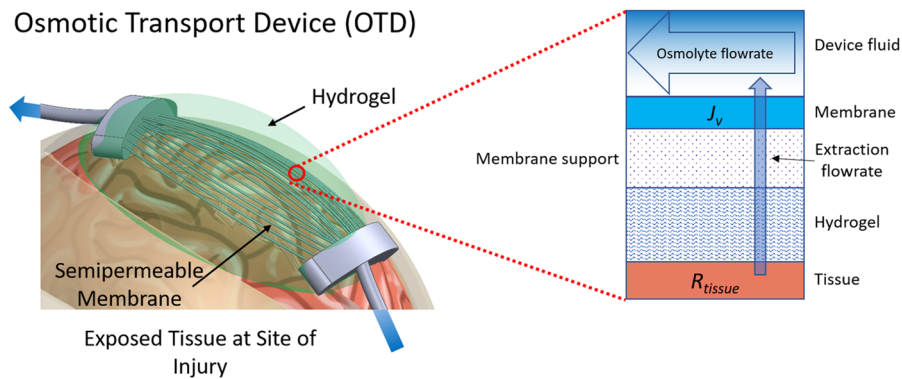


FIG. 1. Illustration of an osmotic transport device (OTD)^{1,2} placed at the dura of a brain with edema after injury. The tissue is exposed after decompressive craniectomy. The device operates as a forward osmosis membrane process and will drive fluid from the tissue into the retained osmolyte solution that is expelled from the device (retentate). The volume of expelled fluid can be several orders of magnitude lower than that of the device solution, making conventional methods for determining membrane flux unsuccessful.

hydrateable hydrogel resistance, R_{tissue} is the hydraulic resistance due to the tissue and μ is the solution viscosity. The feed fluid enters the membrane module and flows tangentially across the membrane surface. This approach helps to reduce the solute boundary layer that is inherent at the membrane surface. In addition, tangential flow allows the system to reach steady-state, as well as making the process controllable. The fluid that does not pass through the membrane and, instead, exits the module is termed the retentate. The permeate is the fluid that passes through the membrane. The transmembrane pressure is defined as

$$\Delta P = \frac{P_{feed} + P_{retentate}}{2} - P_{permeate}. \quad (2)$$

The OTD operates like a forward osmosis process where ΔP must be less than $\Delta\pi_{osmolyte}$ to remove fluid from the tissue. The osmotic pressure is directly coupled to the osmolyte concentration at the membrane surface. Since the permeate flux is reversed, the concentration of the osmolyte at the surface is substantially reduced and this becomes a function of the tangential flowrate of the retentate in the OTD, the initial osmolyte concentration and the total resistances to flow (i.e. $\sum_i R_i$ from Equation (1)). Because of the ultra-low permeate flux inherent to the applications associated with the OTD, a computational modeling analysis is used to estimate the concentration at the membrane surface, determine the net driving force during operation and derive the net permeate flux.

In a typical operation, the volume of fluid extracted from the tissue into the osmolyte solution can be several orders of magnitude lower than the volume of fluid pumped in the OTD. This makes conventional methods of permeate flux measurement ineffective. In this work, we utilize fluid density measurements to measure the ultra-low flow rate of permeate across sample window in the OTD. While many methods exist for measuring fluid density,⁴ most are impractical for this application. For example, hydrometers (weighted glass floats that rise or fall to a location in a fluid that is inversely proportional to the fluid's density) are precision instruments but require large fluid sample volumes that are incompatible with the small volumes of fluid analyzed in this application.^{5,6} Similarly, pycnometers (glass vessels that contain precisely-known volumes) require weighing of discrete volumes of fluid and do not provide the necessary continuous monitoring of solution density.⁷

Vibrating tube sensors were introduced in the 1970s^{8,9} and have since been used in a wide variety of applications, including measuring the density of petroleum,¹⁰ asphalt,¹¹ and engine coolant;¹² measuring the fat content of milk¹³ and the alcohol content of beverages;^{14,15} detecting counterfeit medications,¹⁶ and weighing microgram-sized organisms.¹⁷ In these sensors, a piece of glass tubing is bent into a shape (usually “U” or “W” shaped) and mounted in such a way that part of the tube (the bottom of the “U” or “W”) is free to vibrate. An electronic feedback circuit keeps the tube vibrating at its resonance frequency. When fluid is loaded into the tube, the additional mass of the fluid reduces the effective resonance frequency of the tube. Since the volume of the fluid inside the tubing is constant, this change in resonance frequency is proportional to the density of the fluid.^{8,9} After calibrating the vibrating tube sensor using one or more fluids of known densities, the sensors can be used to measure unknown densities with an accuracy of 0.001 g/mL.¹⁸

The small sample size and high sensitivity of vibrating tube density sensors make them ideal candidates for measuring osmolyte concentration in osmotic transport devices. However, a major limitation for the application of vibrating tube sensors to OTDs is the high sensitivity of the sensors to spurious density changes caused by minute temperature fluctuations. Specifically, typical laboratory temperature variations of a fraction of a degree Celsius over a timescale of a few minutes can result in significant changes in measured sample density, even though the concentration of solute in the sample remains unchanged. This sensitivity to temperature changes is less significant when using these sensors to take a single instantaneous density measurement (which takes only about a second). However, since OTD therapy can take several hours to complete, temperature-induced density fluctuations over this period would generate measurement drift on the order of or greater than the osmolyte concentration changes expected in our tissue permeability measurements.

In this work, we successfully used vibrating tube sensors to quantify ultra-low fluid flux in OTDs. We accomplished this using *differential densimetry*, a novel technique that uses two identical vibrating tube sensors, one upstream of the OTD and one downstream. By measuring the difference between the densities of the fluids upstream and downstream of the OTD, we can calculate the rate of flow of water into or out of the OTD over time. Since any temperature-induced drift in measured density

will affect both sensors equally, differential densimetry is much less sensitive to temperature-induced drift than ordinary density measurement. As a proof of concept, we use differential densimetry with vibrating tube sensors to measure the rate of fluid flow across spinal cord tissue from the rat model via the OTD, *ex vivo*. We also compare our fluid flow measurements with those predicted by finite element simulations of the tissue and membrane systems.

METHODS

Experimental setup

An overview of our differential densimetry method for measuring ultra-low fluid flows through an excised tissue sample via the OTD is shown in Figure 2. The setup allows for two different modes of operation. During “baseline” mode (Figure 2A), rotary valves are set to allow the same osmolyte solution (yellow) to flow through

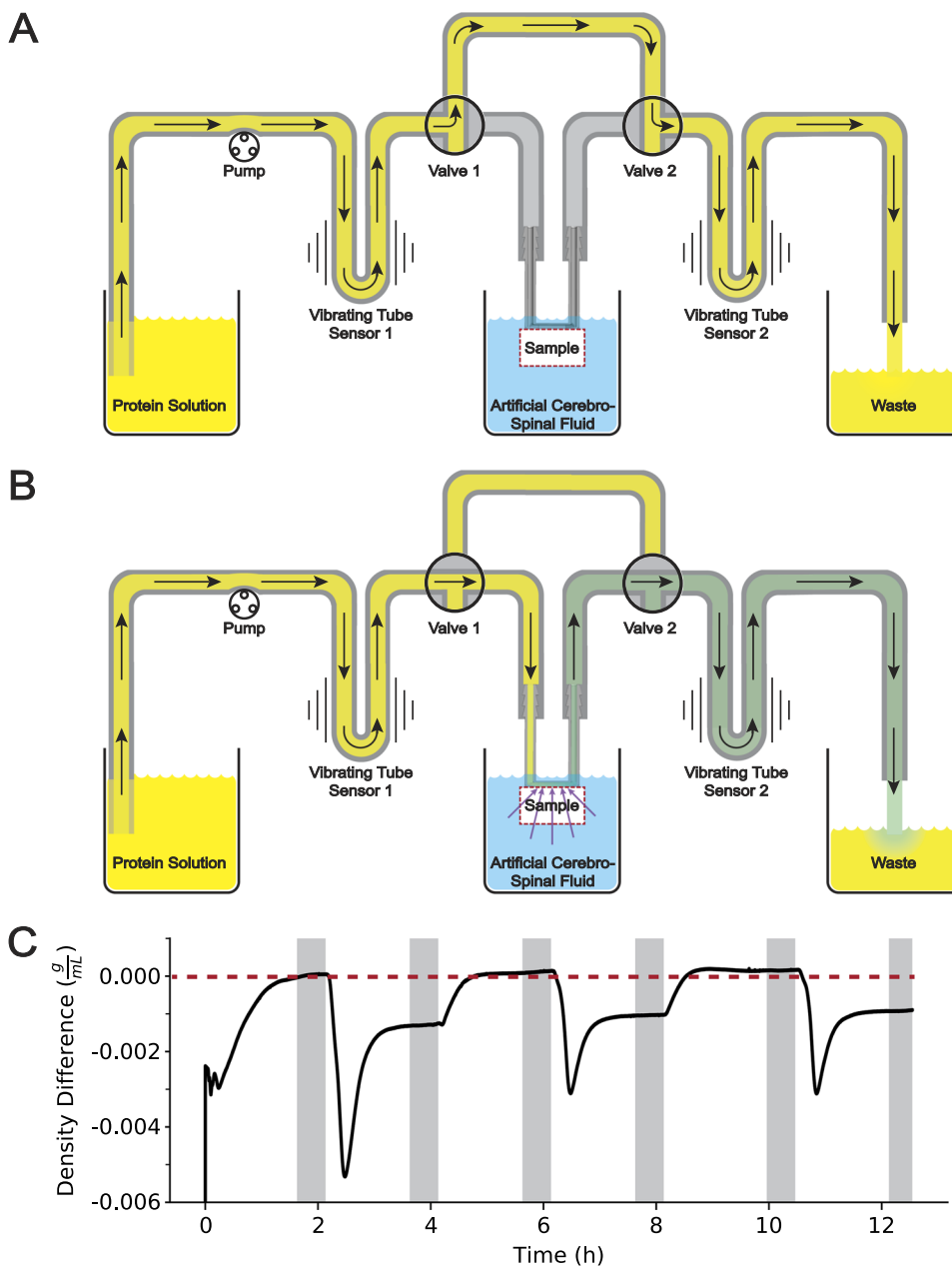


FIG. 2. Overview of the differential densimetry method for measuring fluid flux through a sample mounted to an OTD. During “baseline” mode (A), an osmolyte solution (yellow) is pumped through two vibrating tube density sensors in series, bypassing the sample supported on the OTD. Flowing the same solution through both sensors allows us to calibrate and correct baseline offsets in the sensors. During “run” mode (B), the rotary valves are switched to flow fluid through the OTD and across the top of the tissue sample. Any fluid flowing from the sample into the OTD will modify the osmolyte solution (green) and result in an altered density measurement by the downstream sensor. (C) Illustration of time dependent difference in measured densities between the two sensors for a typical experiment. Transient results are associated with diffusion of solutes throughout the system when the system is closed. Measurements are determined after the process reaches steady-state (area within the grayed regions).

both vibrating tube sensors, without flowing through the OTD and across the sample. This mode allows the sensors to be calibrated with fluid of the same density. During “run” mode (Figure 2B), the rotary valves are set to flow the osmolyte solution through the OTD and across the tissue sample. As the OTD extracts fluid through its membrane, relatively minute amounts of fluid passing through the tissue will combine with the retained osmolyte solution and change the fluid density that is determined downstream of the OTD by the second vibrating tube sensor (green region in Figure 2B).

We used two identical vibrating tube sensors obtained from commercial density meters (Anton-Paar DMA 35 density meters, Graz, Austria). To record the raw resonance frequency of these sensors, we connected the drive coil of each sensor to a frequency counter input on a multifunction data acquisition card in a PC running a custom LabVIEW program (National Instruments, Austin, TX). The resulting data was analyzed by custom Python code that employs low-pass filtering. Fluid was pumped through the device using syringe pumps (Pump 11 Elite, Harvard Apparatus, Holliston, MA) at 100 $\mu\text{L min}^{-1}$ flow rate. Flow was stopped at desired time points to manually switch the flow direction of the rotary valves (EW-30600-02, Cole-Palmer, Vernon Hills, IL).

A molded 0.75 mm thick silicone shell (MED-4901, Nusil, Carpinteria, CA) is added to the membrane device, surrounding the device, except for the area above the membrane. The silicone shell was added to allow for tissue adhesion to the device without potentially adhering to and clogging the device membrane. For consistency, the same silicone was used for all experiments. A 1% (w/w) agar hydrogel was placed on top of the membrane and, if applicable, between the membrane and adhered (VetBond, 3M, St. Paul, MN) rat spinal tissue.

Solution preparation

Experiments were conducted with bovine serum albumin (BSA; No. A30075, Research Products International, Mt Prospect, IL) as the osmolyte in artificial cerebral spinal fluid solvent (aCSF; solutions with composition in mmol/L: Na, 146.5; K, 27.7; Ca, 1.65; Mg, 1.235; Cl, 213.5; P, 0.65)¹⁹ at pH 7.4 and 25°C. Solvent solutions were prepared by dissolving the proper amounts of salts in one liter of reverse-osmosis-purified water. BSA powder was weighed and dissolved in a weighed amount of solvent and gently mixed with a stir bar. For each solution, the pH was adjusted with aliquots of 1 M HCl (No. HX0603, Millipore Sigma, Burlington, MA) and 1 M NaOH (No. S318, Thermo Fisher Scientific, Waltham, MA) while stirring to prevent local denaturation. The solution pH was checked to be within 0.05 pH of 7.4 before use. The amount of acid and base added to adjust the pH was considered part of the solvent and was considered when determining concentrations. Solution concentrations were determined in terms of mass of protein or salt per total volume of solvent.

Density sensor calibration

The vibrating tube density sensors were calibrated with BSA solutions containing varying concentrations of sodium chloride (NaCl) at 21.2°C \pm 0.5°C temperature. Prior to the calibration, the vibrating tube sensors were pre-coated with BSA for 12 h to eliminate variations due to protein adsorption.^{20–23} Following the pre-coating,

three solutions with varying quantities of NaCl (No. S9888, Sigma-Aldrich, St. Louis, MO) were passed through the densimeters over a 35-minute period. The solutions ranged in density from 1.00 to 1.12 g mL⁻¹. The resulting plots of fluid density vs resonance frequency were fitted using linear regressions (Figures S1, S2) to determine each sensor's calibration constants.

Preparing samples for permeability measurement

For measurements of the permeability of an ultrafiltration membrane (NADIR® PM UP010, 10 kDa MWCO, polysulfone, Microdyn Nadir, Wiesbade Germany), a membrane sample with 15 mm² surface area was placed in the membrane holder of the OTD in line between the two density sensors (“Sample” location in Figure 2A) and submerged in a beaker of aCSF. A solution of 350 gL⁻¹ BSA in aCSF at pH 7.4 was driven through tubes via a syringe pump (Harvard Apparatus 11 Plus Syringe Pump, Harvard Apparatus, Holliston, Massachusetts) with an inlet flowrate of 100 $\mu\text{L min}^{-1}$.

For measurements of tissue permeability, an 8- to 10-week-old Sprague Dawley female rat was euthanized by Fatal Plus (DOSE) and cardiac puncture. After expiration, the spinal cord tissue was extracted. The spinal cord tissue was then cut into a 10 mm segment. All experiments were performed with approval from the University of California Animal Care and Use Committee and in accordance with the National Institutes of Health Animal Care and Use Guidelines (AUP#2018-0011).

For measurements of the agar hydrogel permeability, 1% agar by weight was dissolved in aCSF solvent. The agar/aCSF solution was poured into a beaker to achieve the proper gel height (0.75 mm) and then heated for 30 s on high in a microwave. The hydrogel was then removed by spatula and placed above the device membrane in the silicone shell opening of the OTD.

Densimetry measurements

Each experiment began with flow through the bypass path shown in Figure 2A. After approximately 2 hours of flow through the bypass, the 3-way valves were switched to divert fluid flow through the membrane device. After approximately 2 hours of flow through the membrane device, the flow was again switched back to the bypass. This process was repeated three times in order to collect multiple measurements of the fluid flux across the membrane. Steady-state density measurements were averaged for each period of flow through the membrane device and were compared to the average steady-state baseline density measurements.

Calculation of extraction rates

The fluid flux through the membrane was determined by first comparing the density difference, D_D , between the individual sensors. Eq. (3) shows the algorithm uses for the comparison. Here,

$$D_D = S - S_0 + S * \left(1 - \left(\frac{B}{B_0} \right) \right), \quad (3)$$

where S is the signal density of the downstream sensor, S_0 is the initial signal steady state average density, B is the baseline density of the upstream sensor, and B_0 is the initial baseline steady state average density. Next, the fluid extracted rate of the device, V_{S2} , was

TABLE I. Extraction Rates for Densimetry Experiments for Permeable Samples.

Permeable Sample	Extraction Rate ($\mu\text{L hr}^{-1}$) at Evaluation Points (h)		
	2 h	4 h	Avg
Trial 1: OTD membrane only	87.8 ± 1.0	74.7 ± 0.5	81.2 ± 9.7
Trial 2: OTD membrane only	76.0 ± 1.0	69.2 ± 1.3	72.6 ± 4.1
Trial 3: OTD membrane + hydrogel	67.8 ± 1.3	70.7 ± 0.8	69.2 ± 2.1
Trial 4: OTD membrane + hydrogel + tissue without dura		31.5 ± 0.7	
Trial 5: OTD membrane + hydrogel + tissue without dura		33.0 ± 1.0	
Trial 6: OTD membrane + hydrogel + tissue with dura intact		53.9 ± 0.6	

calculated from the density differences and the solution and sensor parameters by relating the parameters as

$$D_D = \frac{\frac{V_P}{SV} + V_{S1} * D_S}{V_P + V_{S1}} - \frac{\frac{V_P}{SV} + D_S(V_{S1} + V_{S2})}{V_P + V_{S1} + V_{S2}}, \quad (4)$$

where V_P is the volume of the protein, SV is the specific volume of the protein, V_{S1} is the volume of solvent initially in solution, and D_S is the density of the solvent. Solving for the volume extracted gives

$$V_{S2} = \frac{D_D(V_P^2 + 2V_P V_{S1} + V_{S1}^2)}{V_P(D_D - (\frac{1}{SV} - SD)) + V_{S1}D_D}. \quad (5)$$

By substituting

$$V_P = \frac{\text{Concentration} * \text{Flowrate} * SV}{1000}, \quad (6)$$

and

$$V_{S1} = \text{Flowrate} - V_P \quad (7)$$

for the volume of protein and volume of initial solvent, respectively, the volume extracted was converted to an extraction rate.

RESULTS

Fluid density measurements vs time

Fluid density measurements vs time for each run illustrated in Figures S3–S8. Sample of steady-state values are shown in Table S1 for Trials 1 and 2. After each switch of the fluid path, we observed

that the density sensors took roughly 1.5 h to reach steady state values. In all experiments, after the 3-way valves were switched to allow fluid through the OTD, there was a significant decrease in the density of the downstream fluid due to the dilution of protein solution from the flux of solvent across the membrane and into the OTD. Additionally, after the valves switched flow through the bypass channel, there was a significant increase in density of the downstream fluid due to undiluted protein solution reaching the sensor.

Extraction rates

The extraction rate results for various configurations for the setup are summarized in Table I. The manufacturer-provided hydraulic permeability for the 10 kDa NADIR[®] PM UP010 membrane used in this study predicts an extraction rate for the OTD to be approximately $100 \mu\text{L h}^{-1}$ if the membrane was used alone and assuming a transmembrane pressure of 14.4 kPa. The computational estimate of the overall pressure drop ($\Delta P - \sigma_{osmolyte} \Delta \pi_{osmolyte}$) was -10 kPa.²⁴ Therefore, our results of $77.0 \pm 9.8 \mu\text{L h}^{-1}$ are consistent with the manufacturer's prediction of membrane performance. The presence of tissue in contact with the membrane substantially reduced the extraction rate. One anomaly is that removing the dura resulted in a reduction in the extraction rate compared to measurements using tissue with dura. Nevertheless, the error in the measurement had a maximum of only 12% (in the OTD membrane only study). This indicates that this method can provide flux measurements with reasonable reproducibility and has the potential to assist in real-time evaluation of fluid removal *in-vivo*.

TABLE II. Hydraulic Resistances Calculated from Measured Extraction Rates.

Sample	Hydraulic Resistance (m^{-1}) $\times 10^{-12}$
OTD membrane only	11.2 ± 1.02
Hydrogel	1.2
Tissue without dura	14.3
Tissue with dura	3.6
Overall Resistance: OTD membrane + hydrogel	12.5 ± 0.04
Overall Resistance: Membrane + Hydrogel + Tissue with Dura Removed	26.8 ± 0.31
Overall Resistance: Membrane + Hydrogel + Tissue with Dura Intact	16.0 ± 0.05

Measurement of hydraulic resistance of tissue

The hydraulic resistance of tissue was also determined using the results from the extraction rate and Eq. (1). Table II shows these results.

The reproducibility of the differential densimetry method is also reflected in determining the various transport resistances of samples. The OTD membrane resistance was determined to be $(11.2 \pm 1.02) \times 10^{-12} \text{ m}^{-1}$. The overall tissue resistance with the dura intact was determined to be $(16.0 \pm 0.05) \times 10^{-12} \text{ m}^{-1}$, or about a 40% increase in resistance as compared to the OTD alone. The process of removing the dura resulted in a 140% increase in hydraulic resistance. It is unclear why the removal of the dura increased the overall resistance and additional studies are required to determine if this is an anomaly or artifact in the method. Nevertheless, the error analysis implies that the differential densimetry method can provide preliminary resistance measurements for subsequent *in-vivo* studies.

DISCUSSION

The system was found to reach steady state values within 1.5 h where the critical measurements are determined (Figures S3-S8). The delay in the system is coupled to the specific overall configuration with the flow lines and flowrates and, thus, it can be reduced. Overall, this short time frame allows for its potential use in real-time applications of an OTD.

Comparing the retentate flowrate ($100 \mu\text{L min}^{-1}$) with the permeate rate, the differential densimetry method shown here was able to determine membrane permeability rates nearly 200 times less than the transmembrane flowrate (observed in Trial 4 at $31.5 \mu\text{L h}^{-1}$, Table I) with a repeatability error as low as 3% (Table I, Trial 2 average) and only as high as 12% (Table I, Trial 1 average). Improved sensitivity could be achieved by modifying the sensors and increasing variation in the density of the two related fluids.

Currently, our differential densimetry method requires milliliter-scale volumes of fluid due to the size of the vibrating tube sensors we are using. This limits the practical utility of our technique in microscale applications, such as in direct animal studies, where sub-microliter flows may need to be measured. For these applications, vibrating tube sensors could be replaced by microfluidic Suspended Microchannel Resonators (SMRs),²⁵ which are capable of continuously measuring fluid density using much smaller fluid volumes. For example, an SMR sensor developed for nanoparticle analysis²⁶ can measure the density of a fluid using only about 20 femtoliters; this is about ten orders-of-magnitude less fluid than vibrating tube sensors require. Performing ultra-low-volume differential densimetry using two SMRs as density sensors would likely require that both SMRs be integrated into the same microfluidic chip, and recent multi-SMR chips (developed for particle and cell analysis) demonstrate that this is indeed feasible.²⁷⁻²⁹ By leveraging microfluidic mass sensors, differential densimetry could be used to measure extremely small fluid fluxes in microscale applications.

CONCLUSION

In this work, we introduced differential densimetry, a method for measuring ultra-low fluid fluxes across tissue *ex-vivo*. By leveraging two density sensors in series, this technique is relatively

insensitive to temperature-induced drift in density measurements which often plague density measurement techniques. As a proof-of-concept, we used differential densimetry to measure the membrane flux of a concentrated BSA solution in aCSF at pH 7.4 moving through across a 15 mm^2 membrane opening of an osmotic transport device (OTD) with a transmembrane flowrate of flowrate of $100 \mu\text{L min}^{-1}$.

The differential densimetry method shown here was able to determine membrane permeability rates over two orders of magnitude less than the transmembrane flowrate. Improved sensitivity could be achieved by modifying the sensors. The system was also found to reach steady state values in less than 2 h where the critical measurements are determined. The system can be easily extended to microscale applications by modifying the process with already existing technology.

For *in-vivo* applications, permeability of tissue and overall system time lag must be established prior to quantifying permeate flux. These preliminary studies for determining permeability and the systems transient operations could be done *ex-vivo*. Overall, the differential densimetry technique provides a convenient and safe method for measuring low flowrate transport through the OTD.

SUPPLEMENTARY MATERIAL

See [supplementary material](#) for S1—Densimeter Calibrations; S2—Densimetry Data Figures.

ACKNOWLEDGMENTS

Financial support from the Craig H. Neilsen Foundation (Project Number 382387) and from the Jacques S. Yeager, Sr. Professorship. Thanks to Jennifer Yang, Vamsi K. Choday and Shivam V. Kardani. In memory of Professor Dimitri Morikis.

The authors declare no competing interests.

REFERENCES

- ¹D. W. McBride *et al.*, "Reduction of cerebral edema via an osmotic transport device improves functional outcome after Traumatic Brain Injury in Mice," in *Brain Edema XVI* (Springer, 2016), pp. 285–289.
- ²D. W. McBride *et al.*, "Improved survival following cerebral edema using a novel hollow fiber-hydrogel device," *Journal of Neurosurgery* **116**(6), 1389–1394 (2012).
- ³O. Kedem and A. Katchalsky, "Thermodynamic analysis of the permeability of biological membranes to non-electrolytes," *Biochim Biophys Acta* **27**(2), 229–246 (1958).
- ⁴S. V. Gupta, *Practical Density Measurement and Hydrometry* (Institute of Physics Publishing, Bristol, 2002).
- ⁵S. Kolupaila, Bibliography of hydrometry, 1961, Notre Dame, Ind., University of Notre Dame Press, xxiii, 975 p.
- ⁶ASTM E100-17, Standard Specification for ASTM Hydrometers, 2017, ASTM International, West Conshohocken, PA.
- ⁷ASTM D1217-15, Standard Test Method for Density and Relative Density (Specific Gravity) of Liquids by Bingham Pycnometer, 2015, ASTM International, West Conshohocken, PA.
- ⁸S. Janssen, Device for measuring the density of a fluid, US, 1973.
- ⁹ASTM D4052-18a, Standard Test Method for Density, Relative Density, and API Gravity of Liquids by Digital Density Meter, 2018, ASTM International, West Conshohocken, PA.

- ¹⁰ ASTM D7777-13(2018)e1, Standard Test Method for Density, Relative Density, or API Gravity of Liquid Petroleum by Portable Digital Density Meter, 2018, ASTM International, West Conshohocken, PA.
- ¹¹ ASTM D8188-18, Standard Test Method for Determination of Density and Relative Density of Asphalt, Semi-Solid Bituminous Materials, and Soft-Tar Pitch by Use of a Digital Density Meter (U-Tube), 2018, ASTM International, West Conshohocken, PA.
- ¹² ASTM D5931-13(2017), Standard Test Method for Density and Relative Density of Engine Coolant Concentrates and Aqueous Engine Coolants by Digital Density Meter, 2017, ASTM International, West Conshohocken, PA.
- ¹³ A. Paar, Technical Note XPAIA001EN-F: The hand in hand solution for milk and dairy products, Graz, Austria, 2019, p. 7.
- ¹⁴ D. H. Strunk, J. W. Hamman, and B. M. Timmel, "Determination of proof of distilled alcoholic beverages, using an oscillating U-Tube density meter," *Journal of the Association of Official Analytical Chemists* **62**(3), 653–658 (1979).
- ¹⁵ F. G. Mark and T. E. Vaughn, "Determination of proof of alcoholic beverages using oscillating U-Tube density meter," *Journal of the Association of Official Analytical Chemists* **63**(5), 970–972 (1980).
- ¹⁶ H. C. Bhakta, V. K. Choday, and W. H. Grover, "Musical instruments as sensors," *ACS Omega* **3**(9), 11026–11032 (2018).
- ¹⁷ S. Mesbah Oskui *et al.*, "Measuring the mass, volume, and density of microgram-sized objects in fluid," *PLoS One* **12**(4), e0174068 (2017).
- ¹⁸ A. Paar, DMA 35 portable density and concentration meter, Graz, Austria, 2018, p. 5.
- ¹⁹ E. Csenker *et al.*, "Ion concentrations in serum and cerebrospinal fluid of patients with neuromuscular diseases," *Arch Psychiatr Nervenkr* (1970) **231**(3), 251–258 (1982).
- ²⁰ S. F. Oppenheim, C. B. Phillips, and V. G. J. Rodgers, "Analysis of initial protein surface coverage on fouled ultrafiltration membranes," *Journal of Colloid and Interface Science* **184**(2), 639–651 (1996).
- ²¹ Y. Wang and V. G. J. Rodgers, "Free-solvent model shows osmotic pressure is the dominant factor in limiting flux during protein ultrafiltration," *Journal of Membrane Science* **320**(1-2), 335–343 (2008).
- ²² Y. H. Wang and V. G. J. Rodgers, "Determining fouling-independent component of critical flux in protein ultrafiltration using the free-solvent-based (FSB) model," *Aiche Journal* **56**(10), 2756–2759 (2010).
- ²³ Y. H. Wang and V. G. J. Rodgers, "Electrostatic contributions to permeate flux behavior in single bovine serum albumin ultrafiltration," *Journal of Membrane Science* **366**(1-2), 184–191 (2011).
- ²⁴ C. S. Hale, *Applications of Direct Osmotherapy for Spinal Cord Injury and Other Aspects of Crowded Protein Osmotic Pressure* (University of California, Riverside, 2018).
- ²⁵ T. P. Burg *et al.*, "Weighing of biomolecules, single cells and single nanoparticles in fluid," *Nature* **446**(7139), 1066–1069 (2007).
- ²⁶ S. Olcum *et al.*, "Weighing nanoparticles in solution at the attogram scale," *Proc. Natl. Acad. Sci. U. S. A.* **111**(4), 1310–1315 (2014).
- ²⁷ A. K. Bryan *et al.*, "Measuring single cell mass, volume, and density with dual suspended microchannel resonators," *Lab Chip* **14**(3), 569–576 (2014).
- ²⁸ N. Cermak *et al.*, "High-throughput measurement of single-cell growth rates using serial microfluidic mass sensor arrays," *Nat. Biotechnol.* **34**(10), 1052–1059 (2016).
- ²⁹ M. A. Stockslager *et al.*, "Rapid and high-precision sizing of single particles using parallel suspended microchannel resonator arrays and deconvolution," *Rev. Sci. Instrum.* **90**(8), 085004 (2019).